Progress In Electromagnetics Research M, Vol. 86, 17–26, 2019

An Investigation of Dual-Band Dual-Square Ring (DSR) Based Microstrip Antenna for WiFi/WLAN and 5G-NR Wireless Applications

Biswa R. Swain and Ashish K. Sharma*

Abstract—In this work, a compact planar dual-square ring (DSR) microstrip patch antenna is investigated to acquire dual-band resonance with dual-mode excitation for Wi-Fi/WLAN and 5G-NR based wireless applications. This dual-square ring geometry is employed on single layer dielectric, excited through EM coupling by using a quadrilateral feed patch, which offers massive flexibility in impedance matching for dual-band resonance with minimum coupling effects in common excitation and ground plane. This planar DSR structure shows the resonance at 2.4 GHz and 3.7 GHz frequency bands with bandwidths greater than 100 MHz and 200 MHz, respectively and a maximum gain response of 4.3 dBi with VSWR of $\ll 2$. Here the simulation results are verified through experimental results of the fabricated antenna. This proposed antenna design can be configured for Wi-Fi/WLAN application at 2.4 GHz in lower-order resonance mode (TM_{01}) and for 5G-NR application by utilizing the fringing benefits of higher-order mode (TM_{10}) at 3.7 GHz.

1. INTRODUCTION

Wireless communication technology has gained prodigious growth in recent years. Nowadays, the wireless system focuses on portable communication like laptops, mobile phones, smart TV's, and many other handy devices that enormously use Wi-Fi, WLAN, and Wi-MAX links [1, 2]. Recently, 5G communication is grown to cover up the portable communication system which offers high-speed data transmission over the specified band with a higher rate of accessibility [3]. 5G is an emerging technology that enables modern technology like IoT and mobile communication using the fractional 5G-NR (New Radio) N-43 band (3.6 GHz to 3.8 GHz) [4, 5]. Moreover, future communications look forward to the development of the compact device to fulfil the 5G communication need. Since microstrip patch antennas came to the forefront of the research, the modern wireless communication devices exhibit promising RF performance characteristics with compact design for high-frequency applications [6, 7].

Several microstrip patch antenna designs have been proposed since the 1970s to give promising performance for Radio Frequency (RF) communication. Subsequently, in the 1990s efficient multi-band microstrip patch antenna structures were proposed using slot and stacked based configurations to improve radiation characteristics [8]. A dual-band microstrip antenna with Defected Ground Structure (DGS) on a planar patch and double-psi-shaped patch is proposed in [9] for LTE/WLAN application. Smyth et al. [10] proposed a microstrip patch antenna integrated with uniplanar metamaterial-based EBG structure to achieve multi-band performance. In [11], a stacked microstrip patch with reactive impedance surface is designed for ISM/ Wi-MAX application. Another multi-layered stacked annular patch antenna with line feed is designed [12] for Wi-MAX application. A microstrip feed

Received 5 June 2019, Accepted 24 September 2019, Scheduled 7 October 2019
* Corresponding author: Ashish Kumar Sharma (ashishksharma29@gmail.com).
The authors are with the Department of Electronics and Telecommunication, Veer Surendra Sai University of Technology (VSSUT), Burla 768018, India.

line based rectangular patch with the triangular slot is also demonstrated for multiband WiMAX application [13]. However, it uses large size of the ground plane which increases space requirements and limits its application in compact wireless devices. Thereafter, some more investigations on RFID/WLAN/WiMAX antennas have been presented using complicated DGS structures like multi-triangular ground plane [14], where a separated ground with a slot is designed for multi-band characteristics [15]. Several investigations have been demonstrated in the past two decades to achieve multi-band operation. However, these reported designs show structure complexity, poor gain response, and these developed configurations are difficult to realize.

Hence, in this paper, an uncomplicated, high gain, low cost, compact microstrip patch antenna structure is proposed with a unique quadrilateral feed patch for dual-band operation. To demonstrate the compactness and simple design, the proposed antenna design uses a single-layer configuration with single port excitation. The DSR radiating elements, excited through a single quadrilateral feed patch followed by a probe feed, are used to investigate the dual resonance behaviour for Wi-Fi/WLAN/Bluetooth and 5G-NR (N-43 band) mobile communication. Here an optometric study has been carried out to achieve a minimum coupling and radiation disturbance between the DSR elements. The proposed antenna structure primarily resonates at 2.4 GHz, which has a great demand in Wi-Fi/WLAN/RFID/Bluetooth communication systems, and thereafter it also resonates at 3.7 GHz, which is widely used for 5G mobile communication with high data speed. The proposed DSR microstrip patch antenna is designed using IE3D EM Simulator and characterized by Agilent's VNA followed by an anechoic chamber measurement.

This paper is organized as below to commit a better readable form. The configuration and optimization of the single-layer, single-port DSR compact microstrip patch antenna are discussed in Section 2. Section 3 explains the electrical equivalent of the proposed antenna design. A detailed comparison between simulation and measurement results is discussed in Section 4. Finally, Section 5 concludes our investigation of the DSR microstrip antenna.

2. DESIGN OF DUAL-SQUARE RING (DSR) MICROSTRIP PATCH ANTENNA

The layer configuration of the proposed DSR antenna is presented in Fig. 1. A square ring radiator patch is implemented on a single dielectric structure. In this design, a Rogers RT Duroid 4700 series is considered as a dielectric substrate, with a dielectric constant of 2.5, thickness of 1.5 mm, and loss tangent of 0.002. Here the ground plane is designed on the other side of the dielectric.

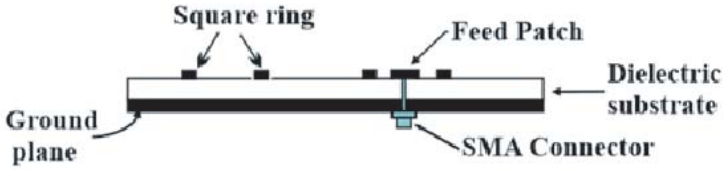

Figure 1. A schematic of layer structure of the proposed Dual-square Ring (DSR) microstrip.

In the beginning, a square patch is designed along with EM coupling excitation through the irregular feed patch. To achieve better performance and less conduction loss, the square patch is replaced by square ring geometry, as shown in Fig. 2. An irregular shape feed patch is modified to a quadrilateral type feed patch in order to improve the impedance matching of the proposed square ring microstrip patch antenna. Here the coaxial feed is connected to the quadrilateral feed patch to excite the square ring microstrip patch. The behaviour of the large and small square rings having side lengths of L_o and L_i are realized with quadrilateral feed patch excitation as shown in Figs. 2(a) and (b). Here the separation gap between the feed patch and inner patch is considered as $g1$, whereas the separation gap between the feed patch and an outer patch is $g2$ as shown in Fig. 2(c). Table 1 shows the design parameters considered for DSR microstrip patch antenna.

The proposed dual-square ring antenna is demonstrated in Fig. 2(c). A suitable separation gap is maintained between the square rings, which is determined with the corresponding wavelength. However,

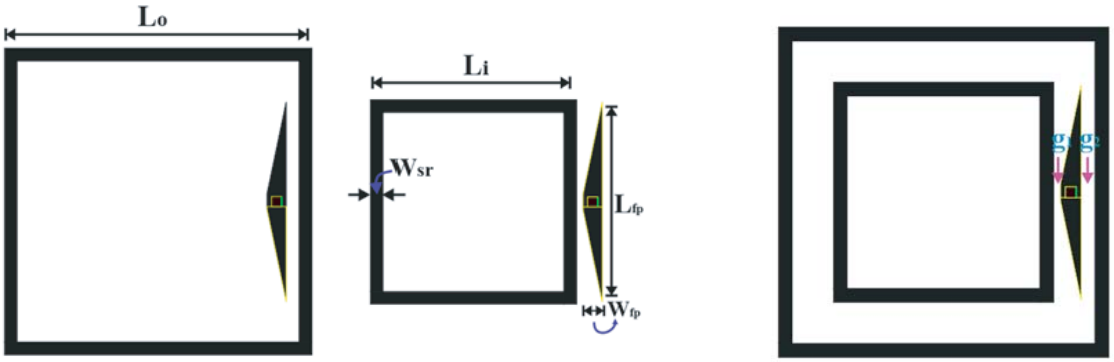

(a) Antenna 1 (b) Antenna 2 (c) Antenna 3

Figure 2. Design of the proposed (a) and (b) single square ring, (c) dual-square ring (DSR) microstrip patch antenna.

Table 1. Design parameters of dual-square ring (DSR) microstrip patch antenna.

Parameters	**Values**
Dielectric constant (ε_r)	2.5
Substrate height	1.5 mm
Loss tangent ($\tan\delta$)	0.002
L_o	24 mm
L_i	15 mm
Ring Width (W_{sr})	1 mm
Feed length (L_{fp})	15.6 mm
W_{fp} (feed length)	1.5 mm
Separation gap (g_1)	0.5 mm
Separation gap (g_2)	1 mm

the iterative study gives the perfect position to achieve dual-band response with a good reflection coefficient parameter. The theoretical analysis can be determined through given mathematical relation;

Altering the physical length can indirectly change the resonances [16]. The clear derivation of the mean perimeter and its effect is well described in [17].

$$\text{Patch length}\,(L)\,\langle\uparrow\rangle\propto mp\,\langle\uparrow\rangle\propto f_r\langle\downarrow\rangle$$
$$\text{Patch length}\,(L)\,\langle\downarrow\rangle\propto mp\,\langle\downarrow\rangle\propto f_r\langle\uparrow\rangle$$

The resonance frequency can be calculated from the relationship below

$$f_r \propto \frac{1}{mp} \tag{1}$$

The electrical size of the radiator patch for a fixed resonance can be determined from equations below

$$f_{r1} = \left(\frac{1}{mp_1} \times \frac{c}{\sqrt{\varepsilon_{eff.}}}\right) \tag{2}$$

$$f_{r2} = \left(\frac{1}{mp_2} \times \frac{c}{\sqrt{\varepsilon_{eff.}}}\right) \tag{3}$$

where 'mp' is the mean perimeter of the square ring structure;

$\varepsilon_{eff.}$ is the effective dielectric constant;

mp_1 is the mean perimeter of the outer square ring;

mp_2 is the mean perimeter of the inner square ring.

3. ELECTRICAL EQUIVALENT OF THE PROPOSED DESIGN

The proposed DSR patch with EM couple feed patch has been analyzed based on cavity model expansion [18], which considers a combination of inductors (L) and capacitors (C). Although a negligible resistance (R) exists, it is ignored in the high-frequency calculation. Therefore, the square rings are replaced by series inductors (Lr1 & Lr2) with series capacitors (Cr1 & Cr2); probe feed patch is replaced by a series inductor (L1) with a parallel capacitor (Cf) edge; the gap between the strips is replaced by series capacitors (Cg1 and Cg2) as shown in Fig. 3.

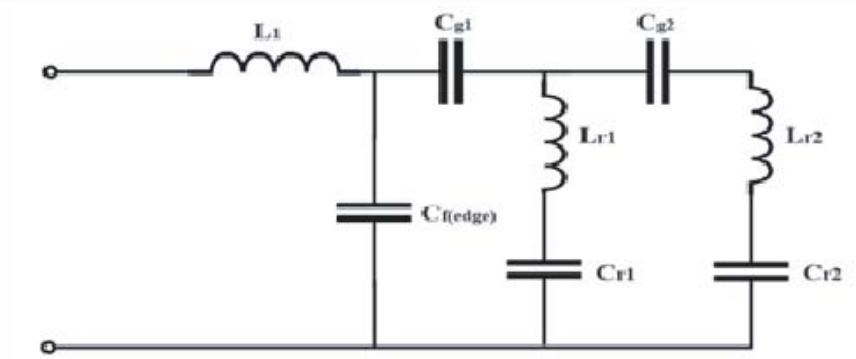

Figure 3. The equivalent circuit of the dual-square ring microstrip patch antenna.

The equivalent impedance can be determined as

$$Z_{in} = Z_f \parallel Z_{r1} \parallel Z_{r2} \tag{4}$$

The equivalent impedance of the feed patch can be determined by

$$Z_f = j\omega L_1 + \frac{1}{j\omega C_{f(edge)}} \tag{5}$$

The equivalent impedance of the inner ring and outer ring can be determined by

$$Z_{r1} = j\omega L_{r1} + \frac{1}{j\omega C_{r1}} \tag{6}$$

$$Z_{r2} = j\omega L_{r2} + \frac{1}{j\omega C_{r2}} \tag{7}$$

The net input impedance of the designed antenna patch can be calculated by

$$Z_{in} = Z_f + \frac{1}{j\omega C_{g1}} + Z_{r1} + \frac{1}{j\omega C_{g2}} + Z_{r2} \tag{8}$$

Using the above equations, the reflection coefficient (Γ) of the designed patch can be calculated as given below. Here, Z_o is the characteristic impedance of the coaxial cable and has a real impedance of $50\,\Omega$.

$$\Gamma = \left(\frac{Z_{in} - Z_o}{Z_{in} + Z_o}\right) \tag{9}$$

Hence, the voltage standing wave ratio (VSWR) can be calculated as

$$VSWR = \frac{1 + |\Gamma|}{1 - |\Gamma|} \tag{10}$$

4. RESULTS AND DISCUSSION

As mentioned, the small square ring of length L_i and the larger square ring of length L_o are designed to operate in 5G-NR bands and Wi-Fi/WLAN Bluetooth based applications, respectively. An optometric

study has been carried out to tune the antenna for specific frequency bands and to realize the multi-mode resonance characteristics. Further, both the individual square ring elements are combined with common excitation and ground plane. The inter-element radiation disturbances and mutual coupling reduction have been taken care of as different excitation modes are realized. The proposed quadrilateral feed patch significantly improves the matching profile of the antenna.

The proposed DSR microstrip patch antenna design is simulated using a full-wave EM solver. The proposed iterative microstrip antenna design is investigated, in which the final prototype with dual-ring yields multi-resonance characteristics as shown in Fig. 4. The S_{11} response shows that the inner square ring with side length L_i (antenna 1) resonates at the higher-order frequency of 3.7 GHz, whereas the outer square ring with side length L_o (antenna 2) resonates at the lower-order resonance of 2.4 GHz. Here it is also observed that the combined geometry of antenna 1 and antenna 2 shows the multi-band resonance at 2.4 GHz and 3.7 GHz with an impedance bandwidth of greater than 100 MHz and 200 MHz, respectively. An optometric study has been carried out by altering the feed position from outside to inside, which shows less impact on the impedance matching profile and reflection coefficient parameter.

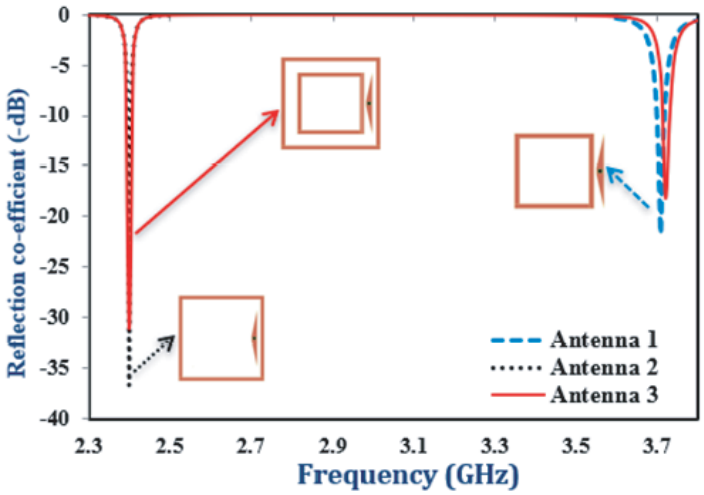

Figure 4. Simulated S_{11} response versus frequency of the proposed antenna design.

In this proposed configuration, coupling effect is also realized from the reflection coefficient plot. Here it is seen that the S_{11} response shows a negligible deviation between single and double square ring structures. Hence, the dual-ring structure delivers almost zero mutual coupling effect between the two rings without affecting the performance of the individual square rings.

To achieve perfect impedance matching in the proposed antenna design, an ideal feed position has been determined through an optometric study. This study considers various separation gaps, as given in Table 2. It shows that the devaluation of the separation gap improves the S_{11} response of the corresponding ring and vice versa. At a certain point of devaluation, the S_{11} response deteriorates to a very small value (less than -10 dB). Hence, decisively the separation gap is chosen as $g1 = 0.5$ mm and $g2 = 1$ mm for better impedance matching.

The resonance effect of the square ring radiator is further realized from the vector current distribution diagram. The vector current distribution at each resonant frequency is observed and plotted in Fig. 5. The current distribution at the first resonant frequency is shown in Fig. 5(a), where it is seen that only the outer ring shows the maximum flow of current responsible for radiation. Similarly, the current distribution at second resonance (3.7 GHz) depicts that only the inner ring has the maximum flow of current distribution as shown in Fig. 5(b).

The fundamental excitation mode of the proposed antenna structure has been realized by considering the patch as a rectangular cavity model, in which the EM waves are confined in the substrate between perfect conductive radiators patch and ground plane, assuming that all side walls are magnetic, where the Transverse Magnetic (TMmn) Mode exists. Theoretically, the excitation mode

Table 2. Optimized values of separation gap between inner and outer square ring.

g_1 (in mm)	g_2 (in mm)	S_{11} at f_{r1} (in dB)	S_{11} at f_{r2} (in dB)
0.3	1.2	−9.5	−11
0.4	1.1	−16	−12
0.5	1	−32	−18
0.6	0.9	−14	−15.5
0.7	0.8	−9	−17

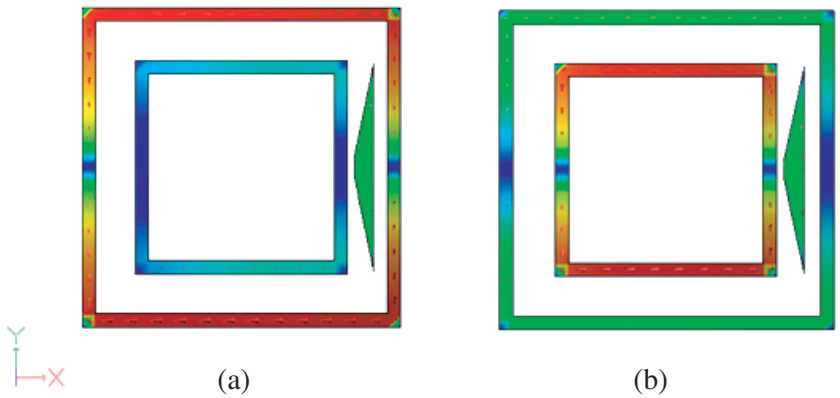

Figure 5. Vector current distribution diagram for proposed dual-square ring microstrip antenna. (a) 2.4 GHz. (b) 3.7 GHz.

can be determined by the standard equation derived by Pozar [19]. Here it is realized that the square ring antenna shows the multi-mode propagation such as TM_{01} and TM_{10}, as identified in Fig. 6. Hence the proposed antenna can be configured to operate at lower-order mode (TM_{01}) for Wi-Fi/WLAN Bluetooth applications and higher-order resonance mode (TM_{10}) for the 5G-NR mobile communication application.

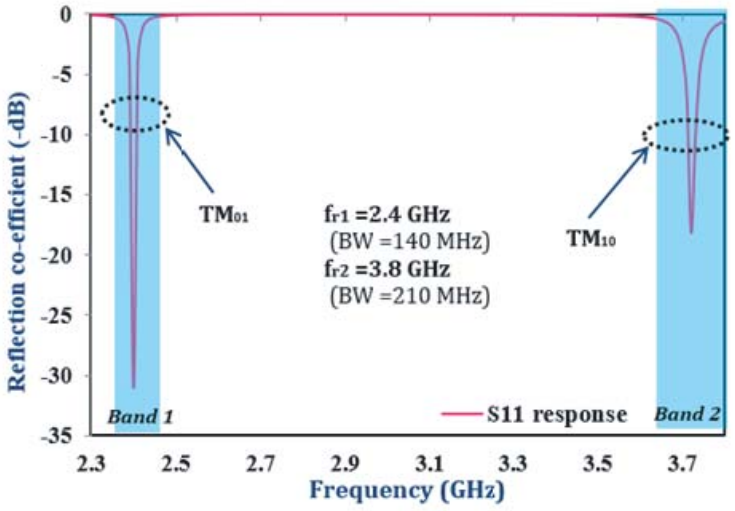

Figure 6. Band identification with fundamental modes for proposed antenna structure.

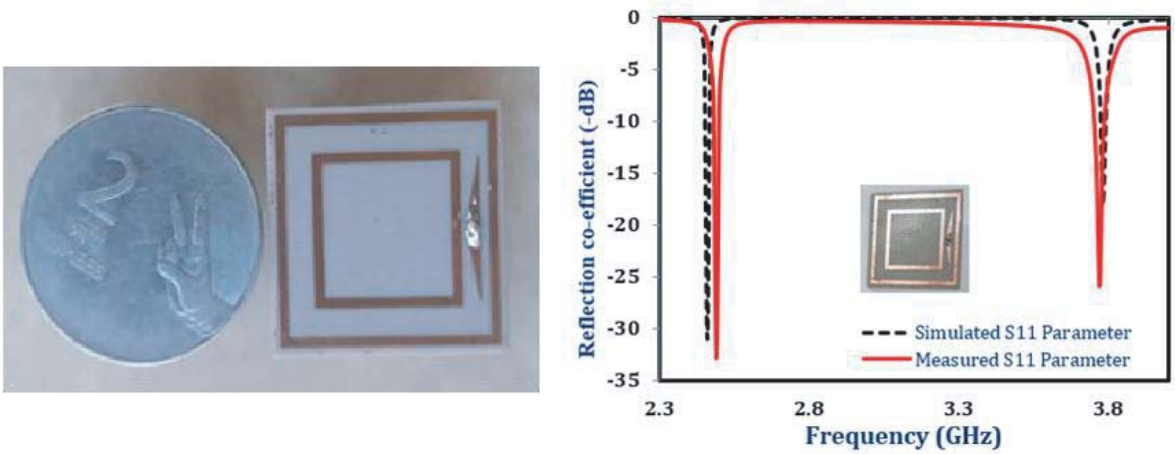

(a) (b)

Figure 7. (a) Fabricated prototype and (b) S-parameter response for dual-square ring (DSR) microstrip patch antenna.

The fabricated prototype of the proposed antenna design is shown in Fig. 7(a), where the top surface shows the proposed dual square ring antenna, and the bottom side shows the ground structure. The fabricated antenna is characterized using the Vector Network Analyzer (VNA), in which the simulated reflection coefficient parameters of the optimized antenna are verified. The measurement of S_{11} response of the fabricated antenna is plotted in Fig. 7(b) along with the simulated result. This figure explains that the measured results are in a good agreement with the simulation ones.

The measured result shows the antenna's first resonance at 2.4 GHz with an impedance bandwidth of 140 MHz (2.34–2.48 GHz). Later, the antenna resonates at 3.7 GHz with an impedance bandwidth of 210 MHz (3.68–3.89 GHz). Moreover, the measured reflection coefficient parameter is well below −25 dB as marked in the solid red line and has a good agreement with simulated results. Thereafter, the VSWR response is analyzed, which is close to 1, as shown in Fig. 8(a). However, a very small deviation is observed in the measured result, which can be ignored as the resonating bands fall very close to the proposed band of operation.

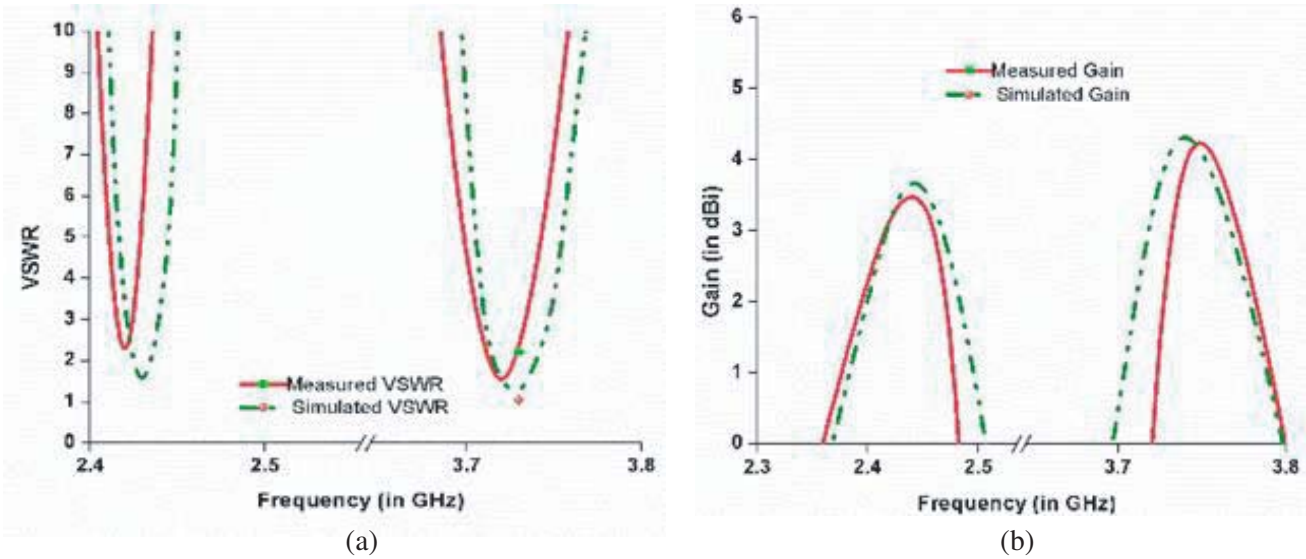

(a) (b)

Figure 8. (a) VSWR response, (b) gain response of the proposed antenna design.

The radiation characteristics of the proposed antenna are measured in a shielded anechoic chamber, and the corresponding results are presented with simulation results. The proposed antenna design shows a maximum gain response of 4.35 dBi and an average gain of around 4 dBi as demonstrated for both the resonant frequencies as shown in Fig. 8(b). It is also observed that the measurement results agree well with the simulation ones.

The radiation pattern of the proposed DSR microstrip patch antenna is measured and plotted in the form of polar charts along with the simulated results, as depicted in Figs. 9 and 10. In this figure,

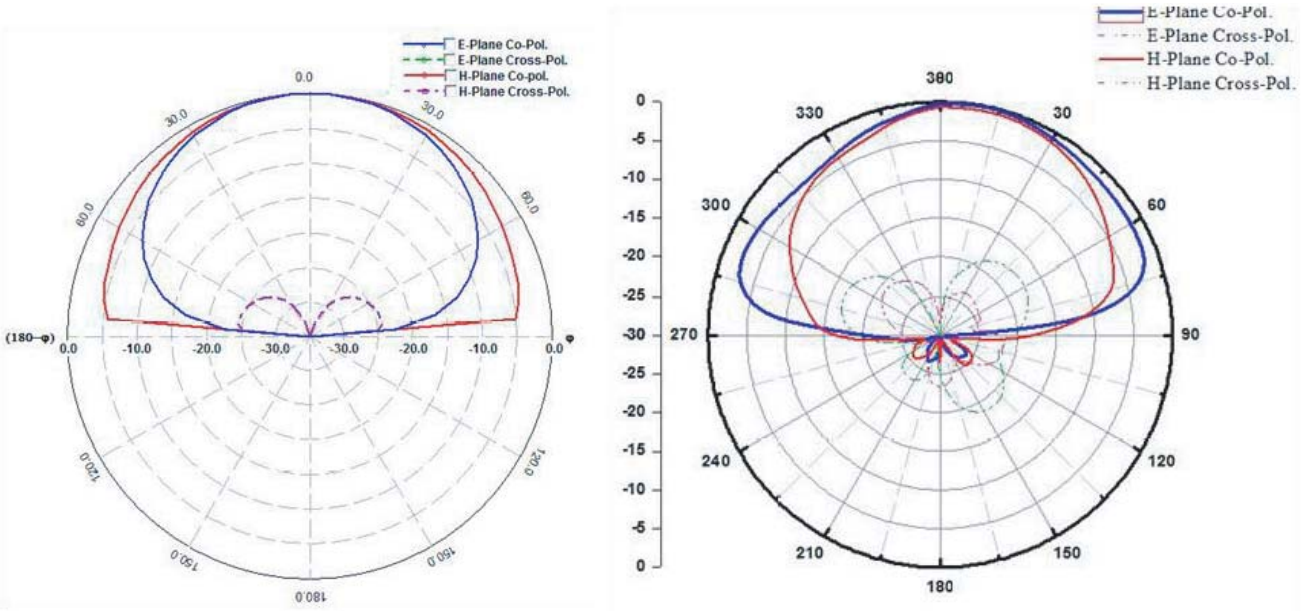

(a) (b)

Figure 9. (a) Simulated and (b) measured radiation pattern of proposed antenna design at 2.4 GHz resonant frequency.

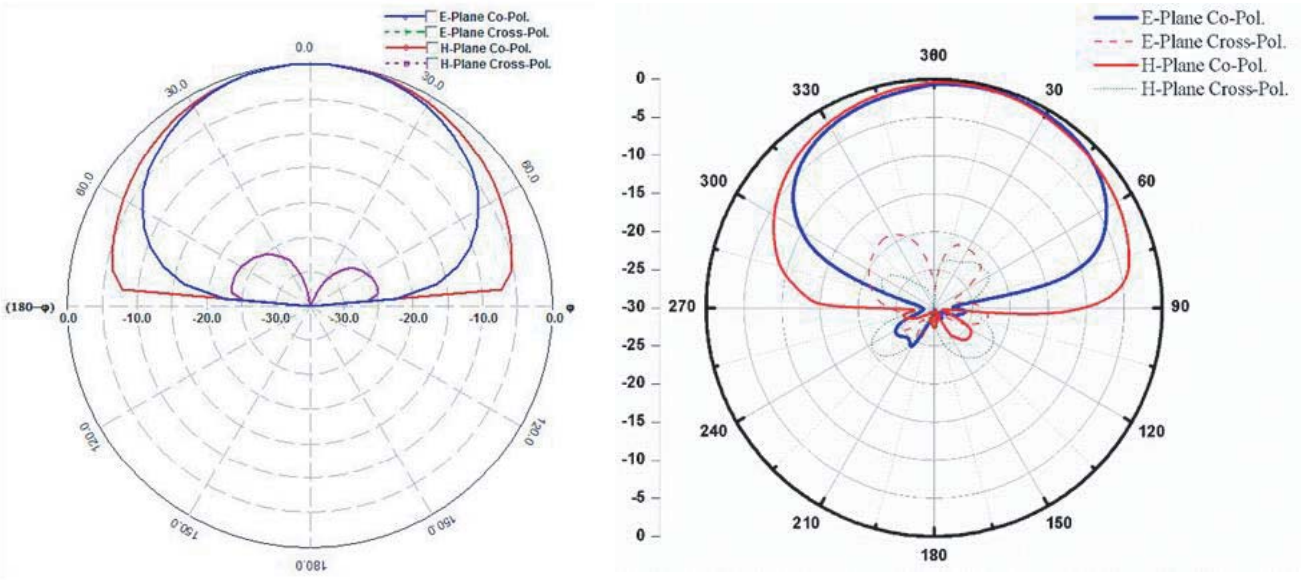

(a) (b)

Figure 10. (a) Simulated and (b) measured radiation pattern of proposed antenna design at 3.7 GHz resonant frequency.

Table 3. Performance comparison of dual-square ring (DSR) microstrip antenna.

Ref.	Size	Technique	Resonances	Gain	Application
Proposed Work	$\mathbf{24 \times 24 \times 1.5\,mm^3}$	***Dual-square ring with quadrilateral feed patch***	***2.4 GHz, 3.7 GHz***	***3.8 dBi, 4.3 dBi***	***WiFi/WLAN, 5G-NR***
[11]	$35 \times 35 \times 5.3\,mm^3$	Stacked Microstrip patch with RIS surface	2.5 GHz, 3.52 GHz	2.93 dBic, 6.26 dBic	ISM/Wi-MaX
[12]	$60 \times 30 \times 21\,mm^3$	Multi-layer, Stacked annular patch	2.5 GHz, 3.5 GHz	1.45 dB, 3.15 dB	Wi-MaX
[13]	$100 \times 92.5 \times 1.54\,mm^3$	Rectangular patch with the triangular slotted ground	2.3 GHz, 3.3 GHz	3.8 dBi, 4.8 dBi	WiMAX/WLAN

the E-plane and H-plane, co-polarization and cross-polarization patterns are measured at both the resonating frequencies. It is realized that the co-polarization patterns show the convergence towards 0 dB, whereas the cross-polarization patterns are well below -25 dB. This depicts that the proposed antenna design has a good linear polarization characteristic. Hence the proposed DSR microstrip patch shows multiband resonance, improved gain, and better impedance characteristics with reduced patch size as compared to the other relevant microstrip patch antenna designs proposed earlier. The performance comparison of the proposed antenna is tabulated in Table 3.

5. CONCLUSION

A compact single layer, dual-square ring (DSR) microstrip patch antenna with a quadrilateral feed patch is demonstrated for Wi-Fi/WLAN and 5G-NR mobile communication. The quadrilateral feed patch with probe feed significantly improves the impedance matching employing EM coupling for dual ring microstrip structure. The proposed antenna shows resonance at 2.4 GHz and 3.7 GHz to acquire its application in Wi-Fi/WLAN, Bluetooth and 5G-NR mobile communication, respectively. This planar ring structure exhibits a maximum bandwidth of 210 MHz and a maximum gain response of 4.3 dBi with VSWR $\ll 2$ for both resonant frequencies. This design shows its efficient performance to overcome coupling effect and interelement radiation disturbances. Moreover, the antenna exhibits TM_{01} and TM_{10} excitation modes for 2.4 GHz and 3.7 GHz resonating frequencies. Owning to these remarkable performances, the antenna is proposed for Wi-Fi/WLAN and 5G-NR mobile communication.

ACKNOWLEDGMENT

The authors would like to thank Mr. Vivek Singh, Scientist at SAMEER Kolkata for his kind support and advice during the antenna characterization and measurements.

REFERENCES

1. Liao, W.-J., S.-H. Chang, and L.-K. Li, "A compact planer multiband antenna for integrated mobile devices," *Progress In Electromagnetic Research*, Vol. 109, 1–16, 2010.
2. Siddiqui, M. G., A. K. Saroj, Devesh, and A. Jamshed, "Multi-band fractaled triangular microstrip antenna for wireless applications," *Progress In Electromagnetic Research M*, Vol. 65, 51–60, 2018.
3. Agiwal, M., A. Roy, and N. Saxena, "Next generation 5G wireless networks: A comprehensive survey," *IEEE Communications Surveys & Tutorials*, Vol. 18, No. 3, 1617–1655, 2016.

4. Kumar, A. and H. Om, "Handover authentication scheme for device-to-device outband communication in 5G-WLAN next generation heterogeneous networks," *Arab. J. Sci. Eng.*, Vol. 43, 7961–7977, Springer, 2018.
5. Goudos, S. K., P. I. Dallas, S. Chatziefthymiou, et al., "A survey of IoT key enabling and future technologies: 5G, mobile IoT, sematic web and applications," *Wireless Pers. Commun.*, Vol. 97, 1645–1675, Springer, 2017.
6. Balanis, C. A., *Antenna Theory Analysis and Design*, 3rd Edition, a John Wiley & Sons Inc. publication, 2003.
7. Garge, R., et al., *Microstrip Antenna Design Handbook*, Artech House, USA, 2001.
8. Antar, Y. M., A. I. Itipiboon, and A. K. Bhattacharyya, "A dual-frequency antenna using a single patch and as inclined slot," *Microwave and Optical Technology Letters*, Vol. 8, No. 6, 309–311, 1995.
9. Voon, C. S., K. H. Yeap, K. C. Lai, C. K. Seah, and H. Nisar, "A compact double-psi-shaped dualband patch antenna for WLAN/LTE applications," *Microwave and Optical Technology Letters*, Vol. 60, 1271–1275, 2018.
10. Smyth, B. P., S. Barth, and A. K. Iyer, "Dual-band microstrip patch antenna using integrated uniplanar metamaterial-based EBGs," *IEEE Transactions on Antennas and Propagation*, Vol. 64, No. 12, 5046–5053, 2016.
11. Agarwal, K. and S. Dutta, "Miniaturized circularly polarized stacked patch antenna on reactive impedance surface for dualband ISM and WiMAX applications," *International Journal of Antennas and Propagation*, Vol. 2015, 1–10, 2015.
12. Shi, W., Z. Qian, and W. Ni, "Dual-band stacked annular slot/patch antenna for omnidirectional radiation," *IEEE Antennas Wireless Propagation Letters*, Vol. 15, 390–393, 2016.
13. Kurniawan, A., I. Iskandar, and M. Prasetiyono, "A 2.3/3.3 GHz dual band antenna design for WiMax applications," *ITB Journal of Information and Communication Technology*, Vol. 4, 67–78, 2010.
14. Tang, Y., W. Gao, J. Gao, and X. Feng, "Compact multi-band printed antenna with multi-triangular ground plane for WLAN/WiMAX/RFID applications," *International Journal of Microwave and Wireless Technologies*, Vol. 8, No. 2, 277–281, 2016.
15. Kumar, P., S. Dwari, and P. S. Bakariya, "Tripple-band microstrip antenna for wireless application," *Wireless Pers. Commun.*, Vol. 96, No. 1, 1029–1037, 2017.
16. Behera, S. and D. Barad, "Circular polarized dual-band antenna for WLAN/Wi-MAX application," *International Journal of RF and Microwave Computer Aided Engg.*, 1–7, Wiley, 2016.
17. Barad, D. and S. Behera, "Hybrid polarized microstrip antenna for multifrequency application," *International Journal of RF and Microwave Computer Aided Engg.*, 1–9, Wiley, 2017.
18. Wolf, E. A., *Antenna Analysis*, Artech House, Norwood, USA, 1988.
19. Pozar, D. M., *Microwave Engineering*, 3rd Edition, a John Wiley & Sons Inc. publication, 2011.